

# Effect of hydraulic and solid ballast on agricultural tractor performance<sup>1</sup>

## Efeito da lastragem hidráulica e sólida no desempenho de trator agrícola

Gabriel Ganancini Zimmermann<sup>2\*</sup>, Daniel Savi<sup>3</sup>, André Carlos Auler<sup>2</sup>, Lauro Strapasson Neto<sup>3</sup>, Samir Paulo Jasper<sup>2</sup>

**ABSTRACT** - The efficiency of the agricultural tractor can be increased with its assertive operational adequacy, ballasting being one of the fundamental factors for obtaining good performance levels, as it is closely related to energy and operational performance. Thus, the objective of this experiment was to evaluate the effect of hydraulic and solid ballast, under different fractions, on the performance of the agricultural tractor. The banded experiment was conducted in a randomized block design, with the treatments consisting of the five configurations of base mass (B0), B0 + 40% hydraulic (HB 40%), B0 + 40% solid (SB 40%), B0 + 75% hydraulic (HB 75%) and B0 + 75% solid (SB 75%), and four target speeds, with five repetitions, totaling 100 experimental units. To determine the efficiency of the tractor, 4 x 2 AFDW with a rated power of 125.2 kW, the parameters of wheel slip, engine rotation, hourly and specific fuel consumption, power, power, and efficiency in the drawbar, operating speed and thermal efficiency of the engine were monitored. The collected data were subjected to analysis of variance/ when significant, submitted to the Tukey test and regression analysis. The obtained results verified that using the hydraulic ballast in the fraction of 75% presented superiority in the energetic and operational performance, highlighting the engine rotation, force in the drawbar, operational speed, and specific fuel consumption. The increase in operational speed can provide gains in energy and operational efficiency; however, it can generate overload on the engine in some ballast configurations.

**Key words:** Agricultural suitability. Fuel consumption. Engine thermal efficiency. Ballast.

**RESUMO** - A eficiência do trator agrícola pode ser acrescida com sua assertiva adequação operacional, sendo a lastragem um dos fatores fundamentais para obtenção de bons níveis de desempenho, pois está intimamente relacionada com o rendimento energético e operacional. Desta forma, o objetivo deste experimento foi avaliar o efeito de lastragem hidráulica e sólida, sob diferentes frações, no desempenho do trator agrícola. O experimento em faixas foi conduzido no delineamento de blocos casualizados, sendo os tratamentos compostos pelas cinco configurações massa de base (B0), B0 + 40% hidráulico (LH 40%), B0 + 40% sólido (LS 40%), B0 + 75% hidráulico (LH 75%) e B0 + 75% sólido (LS 75%), e quatro velocidades, com cinco repetições, totalizando 100 unidades experimentais. Para determinar a eficiência do trator 4 x 2 TDA com potência nominal de 125,2 kW foram monitorados os parâmetros de patinamento dos rodados, rotação do motor, consumo horário e específico de combustível, força, potência e rendimento na barra de tração, velocidade operacional e eficiência térmica do motor. Os dados coletados foram submetidos a análise de variância, e quando significativo, ao teste de Tukey e análise de regressão. Através dos resultados obtidos foi observado que a utilização da lastragem hidráulica na fração de 75% apresentou desempenho energético e operacional superiores, destacando-se as variáveis rotação do motor, força na barra de tração, velocidade operacional e consumo específico de combustível. Verificou-se que o incremento da velocidade operacional pode proporcionar ganho sobre a eficiência energética e operacional, no entanto, pode gerar sobrecarga no motor em algumas configurações de lastragem.

**Palavras-chave:** Adequação agrícola. Consumo de combustível. Eficiência térmica do motor. Lastro.

DOI: 10.5935/1806-6690.20220059

Editor-in-Chief: Prof. Fernando Bezerra Lopes - lopesfb@ufc.br

\*Author for correspondence

Received for publication 26/03/2021; approved on 24/06/2022

<sup>1</sup>Part of the research carried out at the Laboratory of Adaptation of Agricultural Tractors, Universidade Federal do Paraná (UFPR)

<sup>2</sup>Department of Soils and Agricultural Engineering, Universidade Federal do Paraná, Postgraduate Program in Soil Science, Curitiba-PR, Brazil, gabrielganancini@gmail.com (ORCID ID 0000-0002-9709-4458), auler@ufpr.br (ORCID ID 0000-0002-2700-6512), samir@ufpr.br (ORCID ID 0000-0003-3961-6067)

<sup>3</sup>Department of Soils and Agricultural Engineering, Universidade Federal do Paraná, Agronomy, Curitiba-PR, Brazil, daniel.savi98@gmail.com (ORCID ID 0000-0002-2519-0635), laurostrapasson@gmail.com (ORCID ID 0000-0002-9634-3176)

## INTRODUCTION

In recent decades, agricultural tractors have shown meaningful technological progress to meet the increasingly restricted windows of cultivars with short-cycle agronomic characteristics. As a result, research on the adequacy of mechanized sets helps carry out activities with greater operational efficiency and sustainability (LOVARELLI; BACENETTI, 2017).

Operating efficiency is influenced by the relationship between tractor mass and power (SCHLOSSER *et al.*, 2020). With the adequacy of ballast, there are lower energy losses due to rolling resistance and traction, in addition to reducing wheel slippage, operating time, and hourly fuel consumption (DAMANAUSKAS; JANULEVIČIUS, 2015). Most of the studies on the adequacy parameters are from past decades (SHAFAEI; LOGHAVI; KAMGAR, 2018), which do not consider the modern construction projects embedded in these agricultural machines, with the need for further research to meet the productive demand.

Among the types of ballasts frequently used in agricultural tractors, hydraulic and solid ones stand out. Hydraulic ballast consists of adding water inside the tires through calibration valves, allowing parts of the volume previously occupied by air to be replaced by levels of net load. However, to meet the needs of adequacy in conditions in which hydraulic ballast alone is not enough, there is the option of solid ballast, with the use of rings and metal cases intended for fixing on the external side of the wheel-rim and front of the tractor (JANULEVIČIUS; DAMANAUSKAS; PUPINIS, 2018).

Monteiro *et al.* (2013), when studying the operational and energy performance of a tractor using radial and diagonal tires in three conditions of hydraulic ballast (0%, 40%, and 75%), obtained lower slip rates and specific fuel consumption and higher power efficiency in the drawbar with the configuration of 40% and 75% of hydraulic ballast for the radial and diagonal tires, respectively.

Kumar *et al.* (2018) evaluated the effect of ballast on the performance characteristics of the tractor equipped with diagonal and radial tires, using two types of ballasts, hydraulic and solid, and five levels with a base mass of 1050 kg (B0), B0 + 50% hydraulic (B50), B0 + 50% solid (BFe50), B0 + 75% hydraulic (B75) and B0 + 75% solid (BFe75). The authors found that both tires presented the highest operational and energy performance under the BFe75 configuration compared to the other ballasts.

Under field conditions, the adequacy of hydraulic ballast is highly complex and time-consuming compared to the solid equivalent, which is more widespread and convenient for maneuverability, despite the higher aggregate cost (PRNAV; PANDEY, 2008).

In this way, the efficiency of the ballasting operation is closely linked to the energy and operational performance of the mechanized set so that the hydraulic ballast can be more technically and economically accessible in its application. Given the above, the objective of the experiment was to evaluate the effect of different fractions of hydraulic and solid ballast on the operational and energy performance of the agricultural tractor.

## MATERIAL AND METHODS

The study was carried out on a concrete surface, following the rules established by the Organization for Economic Cooperation and Development (2012). The experiment in strips, carried out in a randomized block design, resulted in two types of ballasting (B), hydraulic (HB) and solid (SB), with 0%; 40% HB; 40% SB; 75% HB, and 75% SB allocated in lanes, and the studied speeds (SS) in the plots (4.0, 5.5, 8.0, and 9.3 km h<sup>-1</sup>), totaling 20 treatments. For each treatment, five replications were performed, totaling 100 experimental units.

The tractor used in the experiment was New Holland®, model T7 205, 4 x 2 AFD, rated power (DIN 70030) of 125.2 kW (170 hp), and 18 x 6 Semi-PowerShift® transmission. It was fitted with Goodyear® bias tires model 18.4-26 on the front axle and 24.5-32 on the rear axle, with pressures of 110 kPa (16 psi) and 97 kPa (14 psi). The anticipation of the front wheel about the rear wheel ranged from 2.60 to 3.20% between treatments, obtained according to Schlosser *et al.* (2005). The speeds studied were close to those recommended for intermediate harrowing operation (MARTINS *et al.*, 2018), with the engine speed at 1970 rpm, corresponding to 540 rpm at TDP.

In the 0% treatment, the tractor remained with the original factory mass configuration without adding extra ballast. For treatments with hydraulic ballast, water was added to the four tires up to 40% and 75% levels, respectively. As for the solid configuration, the hydraulic ballast was replaced by iron suitcases containing 45 kg (front) and 65 kg rings (rear) until the mass distribution of the respective treatments with hydraulic ballast was equivalent. The static masses on the tractor axles were determined with a scale (Celmig®) CM-1002, composed of four shoes, as shown in Table 1.

The maximum permissible weight is 10,500 kg, with 4,200 kg on the front axle and 6,300 kg on the rear axle, resulting in a maximum weight allowance of 1,100 kg on the front axle and 1,700 kg on the rear axle.

The experiment was conducted in the convoy method, in which the traction load is provided by changing

**Table 1.** Balancing distribution between the front (F) and rear (R) axles

Ballast	Solid ballast (kg)		Hydraulic ballast (%)		Total mass (kg)		Total mass $\Sigma$ (Kg) *	Mass ratio/Power (kg cv <sup>-1</sup> )
	F	R	F	R	F	R		
0%	630	650	-	-	2.897	4.471	7.368	43.34
40% HB	630	650	40.0	40.0	3.230	5.068	8.576	50.45
40% SB	990	910	-	-	3.416	5.220	8.636	50.80
75% HB	630	650	75.0	75.0	3.965	5.659	9.624	56.61
75% SB	1800	1560	-	-	3.969	5.565	9.534	56.08

\* Mass distribution between axles according to Schlosser *et al.* (2020)

the gear of the second tractor connected to the drawbar, which acts as a brake. The gears used in the first tractor were: 5, 8, 10, and 11, resulting in speeds of 4.0; 5.5; 8.0, and 9.3 km h<sup>-1</sup>. The second tractor operated in gears 2, 4, 6, and 7. The load of 45 kN (4,600 kgf) was selected considering a concrete surface and tractor with 4 x 2 transmission – AFWD, according to ASABE 497.7 (2011). For this purpose, the Magnum 340 model (Case IH®) with a nominal power (DIN 70030) of 234 kW (318 hp) and 18 x 4 Full PowerShift® transmission was used as a brake tractor. During the experiment, both tractors remained with the AFWD activated and the fuel tank full.

The tractor was instrumented with sensors described below. These were connected to the data acquisition system (DAS) with a printed circuit board (JASPER *et al.*, 2016), and the data acquisition frequency of one Hertz was transferred to a hard disk for later tabulation and analysis.

Slippage was determined through engine rotation and tractor displacement speed with and without load, according to Equation 1.

$$SLI = \left(1 - \frac{SL \times RW}{SW \times RL}\right) \times 100 \quad (1)$$

in which,

SLI - wheel slip in %;

SL - tractor displacement speed with load, m s<sup>-1</sup>;

SW - tractor displacement speed without load, m s<sup>-1</sup>;

RL – engine rotation speed with load, RPM;

RW - engine rotation speed without load, RPM.

The engine rotation (ER) was measured from the power take-off (PTO) with the aid of the Autronics® encoder, model E100S. The transmission ratio was obtained using a Victor® digital tachometer, model DM6236P (R<sup>2</sup> = 0.99).

In the fuel supply system (inlet and return to tank), two Flowmate OVAL MIII® flowmeters, model LSF 41L0-M2, were installed, allowing the measurement of hourly fuel consumption (HFC). Consumption was

given by the difference in the number of pulses emitted by the flowmeters and later converted into volume, considering the frequency of 0.001 liters per pulse.

Drawbar force (DBF) was measured using a Bermann® load cell, with a capacity of 100 kN, a sensitivity of 2.0 + 0.002 Mv V<sup>-1</sup>, and a precision of 0.01 kN, properly calibrated and installed on the drawbar attached to the tractor.

To obtain the operational speed (OS), an SVA-60 speed antenna was used, which allows quantifying the displacement as a function of the number of pulses emitted.

The power available on the drawbar was obtained as a function of force and speed, according to Equation 2.

$$DBP = DBF \times OS \quad (2)$$

in which,

DBP – drawbar power, kW;

DBF - drawbar force, kN;

OS - displacement speed, m s<sup>-1</sup>.

From the power available in the drawbar and the tractor engine, it was possible to determine the yield in the drawbar by Equation 3.

$$DBY = \left(\frac{DBP}{EP}\right) \times 100 \quad (3)$$

in which,

DBY - drawbar yield, %;

DBP - drawbar power, kW;

EP - engine power, kW.

The density of the diesel fuel was obtained through the temperatures measured by thermocouples of type K, installed next to the flowmeter in the return of the fuel. Density was determined according to Equation 4.

$$D = (844.14 - 0.53) \times T \quad (4)$$

in which,

D - density of diesel oil, g L<sup>-1</sup>;

T - diesel oil temperature, °C.

844.14 and 0.53 - density regression parameters.

Hourly consumption on a mass basis was determined using Equation 5.

$$HCM = \left( \frac{HFC(844.14 - 0.53 \times T)}{1000} \right) \quad (5)$$

in which,

HCM - hourly fuel consumption based on mass, g h<sup>-1</sup>;

HFC - hourly fuel consumption based on volume, L h<sup>-1</sup>;

1000 - conversion factor.

The specific fuel consumption was determined considering the hourly consumption based on mass, due to the power in the bar, according to Equation 6.

$$SFC = \left( \frac{HCM}{DBP} \right) \quad (6)$$

in which,

SFC - specific fuel consumption, g kW h<sup>-1</sup>;

The engine thermal efficiency was obtained through the specific consumption and the lower calorific value of the fuel by Equation 7, according to Farias *et al.* (2017).

$$ETE = \left( \frac{3600}{SFC \times LCV} \right) \quad (7)$$

in which,

ETE – engine thermal efficiency, %;

LCV – lower calorific value, 42,295 MJ kg<sup>-1</sup>.

The collected data were submitted to the normality test considering asymmetry and kurtosis (MONTGOMERY, 2004); taking into account these premises, they were applied to the analysis of variance to verify the effects of the factors (L and VA) and their interaction, through the statistical program Sigmaplot 12. When the F-test presented a significant probability value ( $p \leq 0.05$ ), the means were compared using the Tukey test ( $p \leq 0.05$ ) for qualitative factors (L). The polynomial regression test was applied to quantitative factors (VE and Interaction), with models selected by the criterion of greater R<sup>2</sup> and significance ( $p \leq 0.05$ ) of the parameters of the equation.

## RESULTS AND DISCUSSION

Table 2 shows the results of the synthesis of the analysis of operational performance data, with no need to transform the averages for all the variables studied. The parameters under evaluation showed a normal distribution because, according to Montgomery (2004), if the asymmetry and kurtosis coefficients are in the range of -2 to 2, the data can be considered normal. In addition,

according to the classification Ferreira (2018), all variation coefficients are categorized as stable, demonstrating stability in the experimental conduct.

All variables showed a significant difference in terms of Ballast and Speed factors studied, denoting their interaction. When analyzing the effect of ballast on the wheel slip variable (SLI), it is observed that its highest levels occurred when operating in the configuration of 0% and 40% SB, corresponding to 8.93 and 8.28%, which exceeded the range of 4 to 8% recommended for concrete surface, according to ASABE D496.3 (2011). However, the use of 40% SB does not differ from 75% HB. The lowest slippage values occurred with the 75% SB configuration, which presented an average of  $1.96 \pm 0.54\%$  less slippage concerning the other configurations, followed by the 40% HB configuration.

Analyzing the different ballast levels, an average reduction in SLI rates of  $0.92 \pm 0.05\%$  is observed with the increase in ballast due to the increase in the interaction between tire and surface, reducing energy dissipation resulting from resistance bearing, according to Šmerda and Čupera (2010). Battiatto and Diserens (2017) emphasize that the slippage index must be defined in an ideal range, with minimum values representing overload on the power train and maximum values indicating energy expenditure.

The 75% HB configuration provided the highest engine rotation (ER) levels, resulting in an average increment of  $159.33 \pm 31.94$  RPM concerning the treatments 0%, 40% HB and 75% SB, and 282 RPM (17.57%) when compared to 40% SB. This result can be explained due to the greater energy demand required with this ballasting configuration, which, through the sensors present in the power train, identified the need to increase the fuel injection by the engine control unit (ECU), consequently increasing the ER.

Regarding the 40% SB configuration, it is observed that the marked reduction in ER can be explained due to the energy expenditure generated with the high SLI without high levels of traction force, so the ECU did not interpret the need for an increase in fuel (MARTINS *et al.*, 2018).

Regarding the different materials used as ballast, it is observed that solid ballast provided a reduction of 0.53 and 0.92 km h<sup>-1</sup> in operating speed (OS) concerning hydraulic ballast in the proportions of 40 and 75%, respectively. This result can be explained by the reduction of the rolling radius with the deformation of the wheelset, which according to Kumar *et al.* (2018), is more pronounced when solid ballast is used than liquid, as the tire casing has greater rigidity when its interior is filled with hydraulic ballast instead of air.

**Table 2** - Statistical synthesis of analysis of variance and test of means for operational performance variables

Analyzes	Evaluated variables			
	SLI (%)	ER (RPM)	OS (km h <sup>-1</sup> )	DBF (kN)
Normality				
Asymmetry	0.02	-1.00	0.52	-1.32
Kurtosis	-0.41	-0.61	-0.17	0.94
F-test				
Ballasting (B)	90.21**	86.25**	116.17**	66.83**
Speed (S)	18.77**	471.92**	493.04**	108.66**
B x S	13.12**	52.54**	60.62**	79.21**
CV (%)				
Ballasting (B)	5.08	2.54	3.31	1.74
Speed (S)	10.54	3.59	4.39	2.63
B x S	7.04	2.53	3.32	2.07
Means Test - L				
B0	8.93 A	1.764 B	5.65 B	43.25 A
HB 40%	7.68 C	1.715 CB	5.51 CB	42.38 B
SB 40%	8.28 B	1.605 D	4.98 D	39.94 D
HB 75%	7.95 B	1.887 A	6.35 A	43.30 A
SB 75%	6.25 D	1.704 C	5.43 C	40.88 C

Variables: wheel slip (SLI), engine rotation (ER), operating speed (OS), and drawbar force (DBF). Analysis of variance F test (ANOVA): NS – Not significant; \* ( $p < 0.05$ ) and \*\* ( $p < 0.01$ ). CV: Coefficient of variation. In each column, for each factor, means followed by the same capital letter do not differ from each other by the Tukey test ( $p < 0.05$ )

Excessive slipping and lower engine speed observed in the 40% SB treatment provided a marked reduction in OS, being  $12.83 \pm 0.06\%$  lower than the other treatments. However, this effect is minimized when using solid ballast in the 75% fraction, resulting in OS values equivalent to hydraulic ballast in the 40% fraction, which does not differ from the treatment without additional ballast. The highest OS observed,  $6.35 \text{ km h}^{-1}$ , occurred in the 75% HB configuration, which according to Serrano *et al.* (2007), can be attributed to the higher ER, which, in turn, determines the rotation regime of the wheelsets through a fixed transmission ratio.

Regarding the drawbar force (DBF), it is observed that the 75% HB configuration presented the highest performance in traction,  $43.3 \text{ kN}$ , resulting in an increase of 8.41 and 5.92% in DBF. About solid ballast in the fraction of 75%, however, it did not differ from the treatment without the addition of ballast. The highest ballast levels, 75% hydraulic and solid, provided an increase of 2.17% ( $0.92 \text{ kN}$ ) and 2.35% ( $0.94 \text{ kN}$ ) of DBF concerning the fractions of 40%, respectively. This is due to the increase in the power mass ratio providing a reduction in energy dissipation and, consequently, an increase in the efficiency of the traction force, according to Šmerda and Čupera (2010).

In general, the hydraulic ballast showed an increase of  $2.43 \text{ kN}$  (6.01%) in the DBF concerning its solid equivalents due to the higher ER observed, which in turn is directly related to the engine speed, indicating a notable increase in the traction on the bar, in agreement with Damanauskas and Janulevičius (2015).

With the analysis of the effect of the studied speeds on SLI, ER, OS, and DBF (Figure 1A-D), a second-order polynomial behavior was observed for all variables, and a coefficient of determination was above 97% in all cases.

Regarding the SLI (Figure 1A), it is observed that, according to the generated equation, the most extraordinary slippage (9.05%) occurred at the speed of  $6.58 \text{ km h}^{-1}$ , noting that between the speeds of  $4.80$  and  $8.40 \text{ km h}^{-1}$ , SLI levels were higher than the 8% recommended by ASABE D496.3 (2011). However, the decrease in SLI when increasing the study speed from  $9$  to  $10 \text{ km h}^{-1}$  is due to the reduction of OS and DBF (KUMAR; NOORI; PANDEY, 2019). These results can be explained by the fact that the skating index is influenced by the selected speeds, according to Monteiro, Lanças and Guerra (2011).

In the ER (Figure 1B), the increase in the speed of interest resulted in its marked reduction; when operating at the studied speeds of  $8$  and  $9.3 \text{ km h}^{-1}$ , a reduction

of 15.1 and 32.5% in the ER is observed, respectively, concerning the lowest speeds, 4 and 5.5 km h<sup>-1</sup>, which do not differ statistically. This result occurs due to the increase in the traction force demand at higher speeds, which, consequently, increases the load on the engine and thus reduces its rotation regime (SERRANO *et al.*, 2007).

Analyzing the operational speed (Figure 1C), this reduction of 0.22 km h<sup>-1</sup> (3.37%) can be observed when the study speed increases from 8 to 9.3 km h<sup>-1</sup>. This is due to the decline in ER due to the increase in traction loads at high speeds, which, simultaneously with the SLI, influence the operational and energy efficiency indices (DAMANAUSKAS; JANULEVIČIUS, 2015).

As for the drawbar force (DBF), Figure 1D, greater traction capacity is observed when operating at a speed of 5.78 km h<sup>-1</sup>, according to the generated equation, which was superior to the DBF of speeds of 4, 8, and 9.3 km h<sup>-1</sup> by 3.5%, 5.4%, and 13.6%, respectively. The lower SLI index can provide this result, indicating an increase in

the contact interaction of the tire with the surface, which consequently promotes a notable increase in traction on the drawbar, as explained by Battiato and Diserens (2017).

Based on the significance of the interaction between the Weighting and Speed factors of interest on the SLI, ER, OS, and DBF variables, we sought to generate equations capable of describing their behavior with a significant coefficient of determination (Figure 2A-D).

Analyzing the effect of the speeds studied in the different ballasting on the SLI variable (Figure 2A), a more significant variation is observed in the treatment without the addition of ballasting due to the tire-ground interaction. Most of the treatments exceeded the limit of 8% of SLI for concrete surfaces when operating at the two intermediate speeds, except for the treatment of 75% HB, which presented for all speeds the slippage between 4 and 8%, within the ideal (BATTIATO; DISERENS, 2017) because excess slipping indicates increased energy expenditure of the mechanized set.

**Figure 1 -** Regression analysis for the isolated speed factor

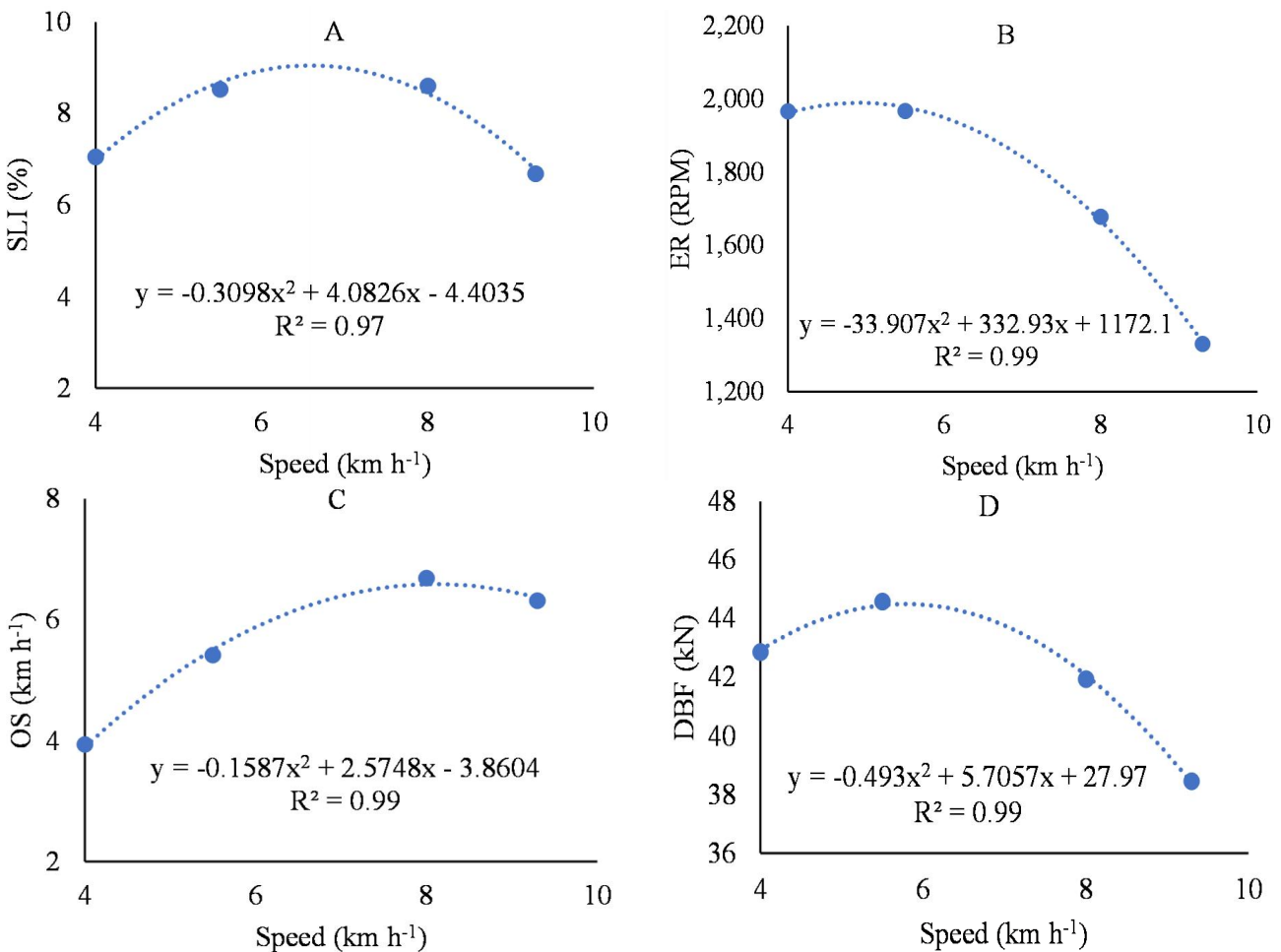
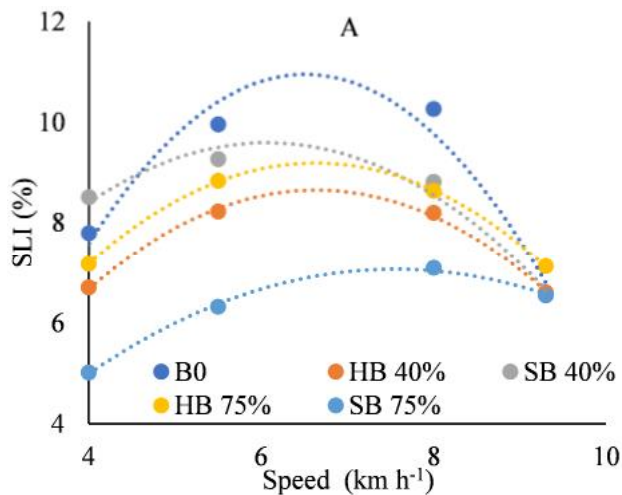
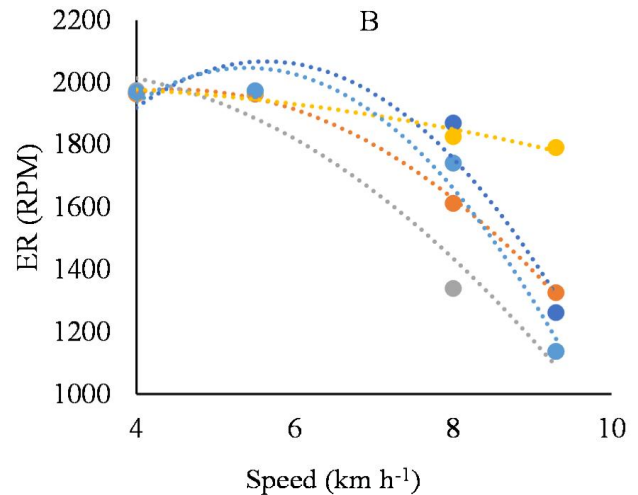


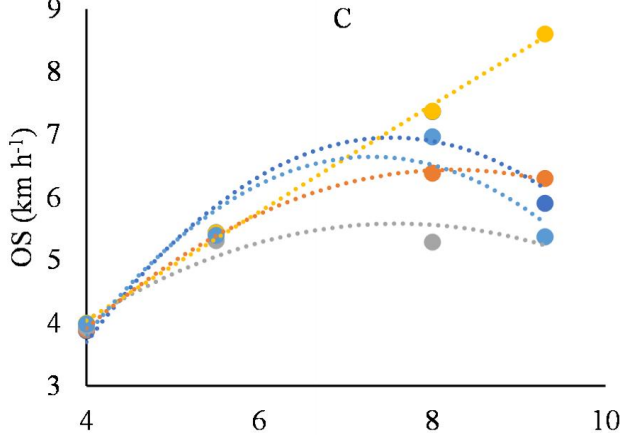
Figure 2 - Regression analysis for the interaction between ballasting and speed



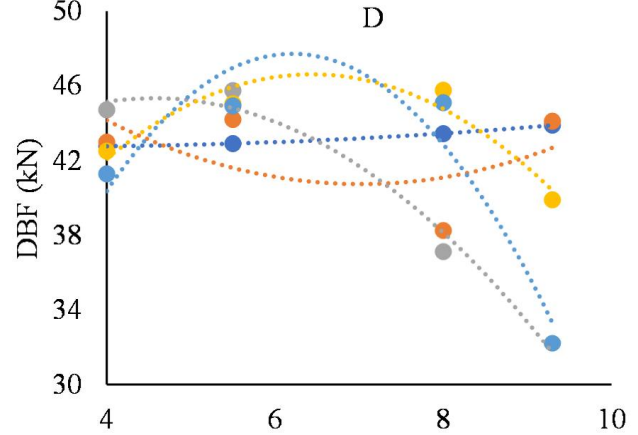
SLI ballast a	$a \cdot V^2$	$b \cdot V$	$c$	$R^2$
SLI B0	$-0.5324V^2$	$6.9339V$	$-11.625$	0.94
SLI HB 40%	$-0.2831V^2$	$3.7587V$	$-3.8268$	0.99
SLI SB 40%	$-0.2788V^2$	$3.3825V$	$-0.6697$	0.96
SLI HB 75%	$-0.289V^2$	$3.8319V$	$3.5153$	0.99
SLI SB 75%	$-0.1645V^2$	$2.4855V$	$2.3147$	0.99



ER ballast	$a \cdot V^2$	$b \cdot V$	$c$	$R^2$
ER B0	$-55.746V^2$	$628.36V$	$296$	0.91
ER HB 40%	$-28.536V^2$	$256.92V$	$1397.7$	0.99
ER SB 40%	$-23.257V^2$	$135.11V$	$1843.9$	0.96
ER HB 75%	$-4.2002V^2$	$18.448V$	$1969.6$	0.94
ER SB 75%	$-57.12V^2$	$616.77V$	$381.21$	0.96



OS ballast	$a \cdot V^2$	$b \cdot V$	$c$	$R^2$
OS B0	$-0.2603V^2$	$3.9245V$	$-7.8378$	0.92
OS HB 40%	$-0.1407V^2$	$2.3169V$	$-3.0956$	0.99
OS SB 40%	$-0.1193V^2$	$1.8118V$	$-1.2929$	0.88
OS HB 75%	$-0.0048V^2$	$0.9148V$	$0.4611$	0.99
OS SB 75%	$-0.2617V^2$	$3.818V$	$-7.2767$	0.89



DBF ballast	$a \cdot V^2$	$b \cdot V$	$c$	$R^2$
DBF B0	$0.0315V^2$	$-0.2083V$	$43.097$	0.99
DBF HB 40%	---	---	---	NS
DBF SB 40%	$-0.6066V^2$	$5.5326V$	$32.708$	0.98
DBF HB 75%	$-0.7555V^2$	$9.7281V$	$15.277$	0.89
DBF SB 75%	$-1.5024V^2$	$18.649V$	$10.172$	0.89

The increase in the study speed resulted in a marked reduction in the engine rotation regime (Figure 2B), regardless of the ballasting configuration used. This is due to the increased energy demand and, consequently, the load on the engine when operating at higher speeds. However, the 75% HB arrangement

showed greater efficiency in ER maintenance, possibly due to the conservation of kinetic energy accumulated in the ballast. The other configurations resulted in rotation regimes between 1326 and 1132 RPM when operating at the desired speed of 9.3 km h<sup>-1</sup>, demonstrating overload in the mechanized set and inability to pull the load of interest,

as well as when operating at the speed of 8 km h<sup>-1</sup> and 40% SB, 40% HB and 75% SB. These rotation regimes lower than the torque reserve can compromise the longevity of the power train due to overload on the drive components (SERRANO *et al.*, 2007).

Analyzing the effect of the studied speeds in the different ballasting on the operational speed (Figure 2C), it is observed that in the configurations 40% SB, 40% HB, 75% SB, and L0, there was no maintenance of the study speed. As a result of the reduction in ER with increasing speed. Regarding the force on the drawbar (Figure 2D), it is observed that the 40% HB configuration did not show a trend as a function of the studied speed, so the mathematical models are not able to explain this factor with a significant coefficient of determination since the other configurations are represented in more than 89% of the cases by the generated equations. With this, it is evident the inability to pull the desired load at a speed of 8 km h<sup>-1</sup> when using ballast in the fraction of 40%, solid and hydraulic, as well as the configurations 40% and 75% LS when operating at the speed of 9.3 km h<sup>-1</sup>. This result can be explained due to the sharp reduction in ER and OS, so the engine traction power in these ballast conditions and speeds becomes lower than the load dem, limiting the traction capacity and, consequently, a sharp drop in DBP.

Table 3 shows the results of the synthesis of the analysis of energy performance data, with no need to transform the averages for all the variables studied, denoting the normal distribution of data according to Montgomery (2004). All coefficients of variation are categorized as stable, according to the Ferreira classification (2018), demonstrating stability in the experimental conduct.

Most variables showed a significant difference in the factors ballast and study speed, except for the hourly fuel consumption (HFC), which did not show a distinction as a function of the ballast factor, denoting the interaction between the factors for all variables evaluated.

Regarding the drawbar power (DBP), it is observed that the 75% HB treatment provided the highest levels, corresponding to an additional 13.93 kW concerning its solid equivalent, which does not differ from the treatment of 40% HB. These results can be attributed to the higher DBP and OS operating in the 75% HB configuration. When analyzing the treatment with the lowest DBP, obtained in the 40% SB configuration, energy expenditure of 13.24 kW is observed concerning the non-use of ballast due to the sharp reduction in the engine speed regime in this treatment, which hampered the maintenance of desired speed. However, the 75% SB and 40% HB configurations showed dissipations

**Table 3** - Statistical synthesis of analysis of variance and test of means for energy performance variables

Analysis	Evaluated variables				
	DBP (kW)	DBY (%)	HFC (L h <sup>-1</sup> )	SFC (g kW h <sup>-1</sup> )	ETE (%)
Normality					
Asymmetry	0.42	0.42	0.25	-0.52	1.28
Kurtosis	-1.04	-1.04	-0.98	-0.61	0.95
F-test					
Ballasting (B)	198.25**	198.27**	2.91NS	19.17**	24.77**
Speed (S)	411.57**	411.48**	125.57**	57.41**	74.91**
B x S	102.47**	102.46**	11.38**	14.15**	16.04**
CV (%)					
Ballasting (B)	3.41	3.41	9.19	8.37	8.70
Speed (S)	4.46	4.46	6.64	8.52	8.94
B x S	3.69	3.69	7.43	7.70	9.10
Means Test - L					
B0	67.99 B	50.79 B	23.37	300 C	29.27 A
HB 40%	64.62 C	48.27 C	22.54	309 BC	30.25 A
SB 40%	54.75 D	40.90 D	23.52	363 A	23.56 B
HB 75%	76.05 A	56.81 A	25.06	293 C	30.26 A
SB 75%	62.12 C	46.40 C	24.05	339 AB	28.78 B

Variables: drawbar power (DBP), drawbar efficiency (DBY), hourly fuel consumption (HFC), specific fuel consumption (SFC), and engine thermal efficiency (ETE). Analysis of variance F test (ANOVA): NS – Not significant; \* (p < 0.05) and \*\* (p < 0.01). CV: Coefficient of variation. In each column, for each factor, means followed by the same capital letter do not differ from each other by the “Tukey test” (p < 0.05)

of 8.63 and 4.95% in DBP compared to the absence of ballast (0%). This can be explained by the engine power being degraded as a function of the active traction efficiency, in which the 75% HB configuration showed superiority in dispatching the available power for traction, corroborating Serrano *et al.* (2007).

Due to the increase in traction power when using hydraulic ballast in the fraction of 75%, greater efficiency of the power train is observed, resulting in the transformation of 56.81% of the engine power into work, 6.02% higher than the treatment without the addition of ballast. However, the 40% HB, 40% SB, and 75% SB configurations resulted in a reduction in the drawbar yield (DBY), which was 2.52, 9.89, and 4.39% lower than the treatment without the use of ballast, respectively. What differs from the authors Monteiro, Lanças, and Guerra (2011) when they report that using different ballasting conditions makes it possible to increase the yield in the drawbar.

The configuration of 40% SB presented a value of specific fuel consumption (SFC) higher than the treatments of 75% HB, 0%, and 40% HB, requiring 19.28%, 17.35%, and 14.87% more than fuel to generate 1 kW h<sup>-1</sup>. Therefore, the 75% SB treatment resulted in an increase of 46 g kW h<sup>-1</sup> concerning its hydraulic equivalent, expressing superior efficiency of the 75% HB configuration in transforming the energy contained in the fuel into work, according to Mayet *et al.* (2019).

Regarding the thermal efficiency of the engine (ETE), the use of the calorific value of the fossil fuel can be observed with the use of the 75% HB treatment, which did not differ from 40% HB and 0%. Still, the use of solid ballast resulted in a reduction in ETE. This evidences the superiority of hydraulic ballast over solid ballast, which, according to Ahmadi (2013), is due to the reduction in the center of gravity of agricultural tractors, which consequently provides more excellent stability of the traction coefficient.

Analyzing the isolated effect of the study speeds on the variables, the second-order polynomial behavior is observed for DBP, DBY, HFC, and ETE, and linear for SFC, both with a coefficient of determination greater than 93% (Figures 3A-E).

Analyzing the isolated effect of the studied speed on the DBP (Figure 3A), it is verified that the highest traction power (78.06 kN) occurred at 7.43 km h<sup>-1</sup>, with a decrease in DBP when operating at the speed of 9.3 km h<sup>-1</sup>, since DBP is influenced by ER, OS, and DBF (LOPES *et al.*, 2019). The highest levels of DBP demonstrate an increase in efficiency during the transformation of mechanical energy into work, which increases over the DBY. The DBY (Figure 3B) showed a performance of 58.3%

when operating at the speed of 7.43 km h<sup>-1</sup>; this result was 7.1% and 11.91% higher than that obtained at the studied speeds of 6 and 9.3 km h<sup>-1</sup> and 40.55% higher when compared to the speed of 4 km h<sup>-1</sup>.

As for the hourly fuel consumption (HFC), Figure 3C shows an increase in the volume demanded when the speed is increased by up to 8 km h<sup>-1</sup> due to the greater energy demand when performing work in a shorter time interval. However, HFC decreased when operating at 9.3 km h<sup>-1</sup> due to the sharp decline in ER. According to Martins *et al.* (2018), the reduction in fuel consumption when operating at lower speeds comes from the lower loss of internal energy.

Due to the non-equivalent behavior between fuel consumption (HFC) and drawbar power (DBP) with increasing speed, a linear reduction in SFC is observed (Figure 3D) to the detriment of the selected speed. According to the generated equation, the fuel demand needed to generate 1 kW h<sup>-1</sup> reduces by 18.70 g with an increase in speed by 1 km h<sup>-1</sup>. Low values of specific fuel consumption at higher speeds studied mean simultaneous optimization of engine performance, traction efficiency and the adequacy of the implementation to the energy supply, and increased operational efficiency (LACOUR *et al.*, 2014).

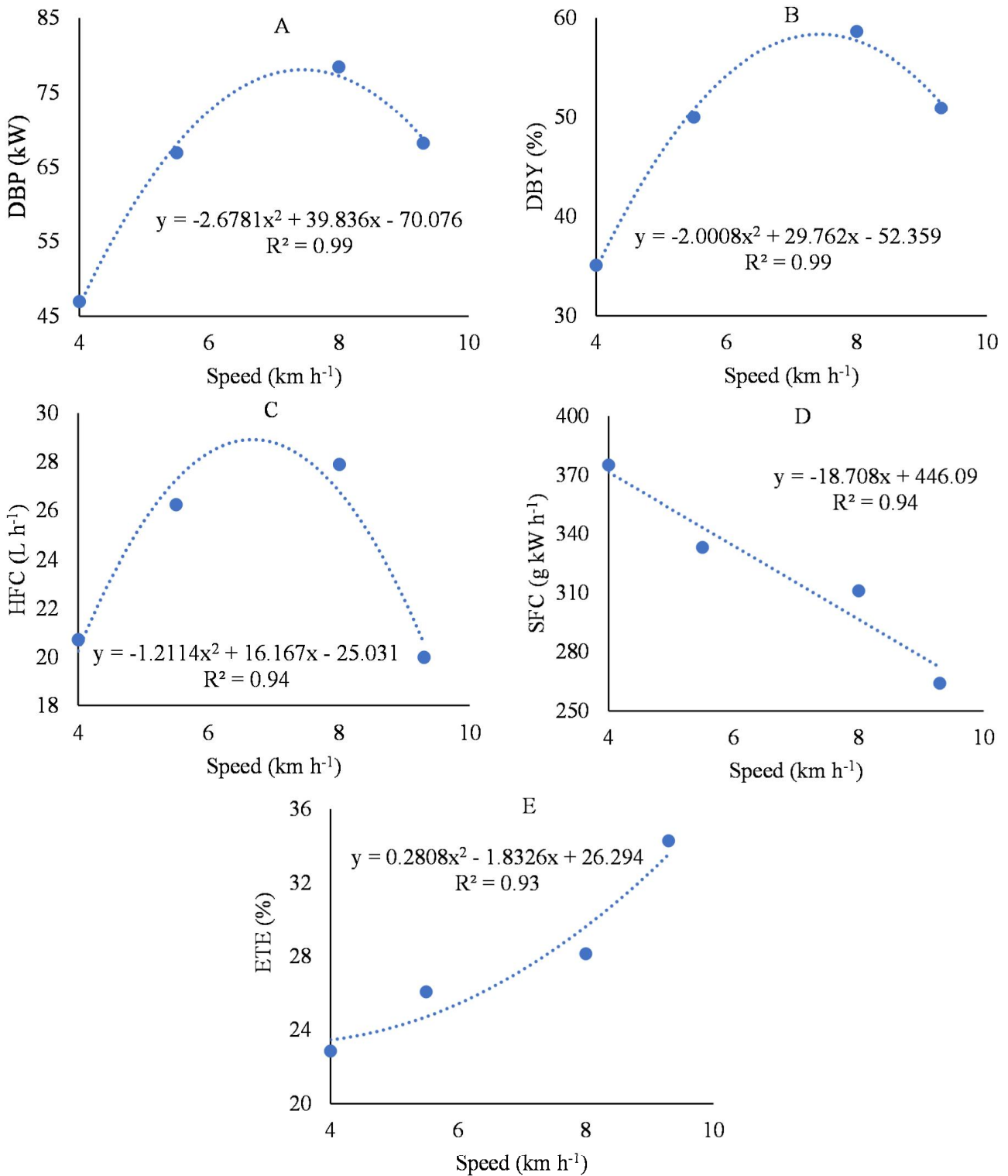
This reduction in SFC, to the detriment of speed, provided an increase in ETE (Figure 3E), which reached the use of 34.27% of the calorific value of the fuel when operating at a speed of 9.3 km h<sup>-1</sup> due to the reduction of sharp ER and HFC at this selected speed. It is noted that this more efficient use of fossil fuels is essential for developing sustainable agriculture (BIETRESATO *et al.*, 2015).

As shown in Table 3, there was a significant interaction between the factors Weighting and Speed studied on the variables DBP, DBY, HFC, SFC, and ETE. Therefore, we sought to generate equations that describe the behavior of these energy performance results with a significant coefficient of determination (Figure 4A-E).

Regarding the traction power (Figure 4A), it is observed that at the lowest speeds studied, 4 and 5.5 km h<sup>-1</sup>, the DBP values do not distinguish between the ballast configurations; however, when evaluating the highest speeds, there is a distinction between treatments. With this, the behavior of non-linear growth for hydraulic ballasts is identified, exceptionally, when used in the fraction of 75% HB since the solid ballast presents a DBP growth of up to 7.0 km h<sup>-1</sup>, according to the generated equations.

The increasing behavior of the DBP in the 75% and 40% HB configurations provided higher levels of DBY with the increase in the target speed (Figure 4B), demonstrating greater efficiency regarding the use of the maximum power available by the engine. On the other hand, the solid configurations showed

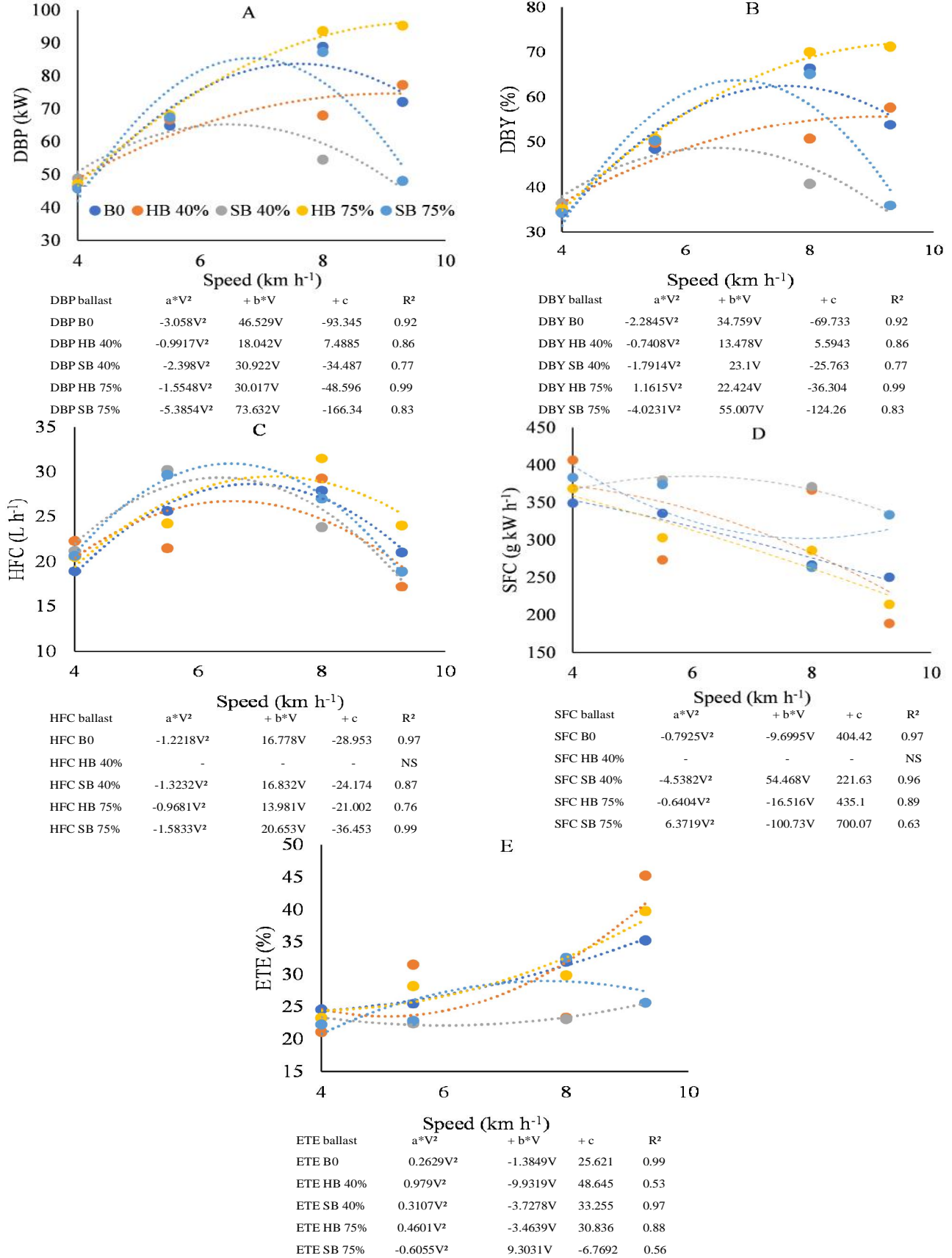
**Figure 3 -** Regression analysis for the isolated speed factor



an increase in DBY when the speed was increased by up to 7.0 km h<sup>-1</sup> due to the marked reduction in ER, OS, and DBF at higher speeds. This corroborates with

Moinfar *et al.* (2020) by demonstrating that energy use is directly influenced by the engine rotation regime and traction load.

Figure 4 - Regression analysis for the interaction between ballasting and speed



As for the hourly fuel consumption (Figure 4C), a second-order polynomial behavior is observed in most treatments, except for 40% HB, which cannot be explained through mathematical models with a significant coefficient of determination. The HFC showed an increase in the volume demanded by increasing the speed by up to 8 km h<sup>-1</sup> due to the greater energy demand when performing work in a shorter time interval. However, both treatments showed a prominent reduction in HFC when operating at the desired speed of 9.3 km h<sup>-1</sup>, which can be explained by the sharp decrease in ER and OS.

Due to the influence of the factors evaluated on the HFC and DBP, the SFC showed a marked tendency to decrease in detriment to the increase in speed, except for the solid ballast arrangements, which presented high values of SFC (Figure 4D), in addition to 40% HB that cannot be explained through mathematical models. Regarding the 75% SB configuration, it is observed that the specific fuel consumption tends to decrease; however, due to the overload when operating at the speed of 10 km h<sup>-1</sup>, the efficiency of fuel use is drastically impaired.

The increase in specific fuel consumption means a simultaneous decline in engine performance, traction efficiency, and the adequacy of the implement to the energy supply, besides the increase in operating efficiency (LACOUR *et al.*, 2014).

The lower SFC leads to more efficient use of the calorific value of fossil fuels and, therefore, results in higher ETE (Figure 4E). The 75% HB configuration had the most prominent ETE concerning the other treatments due to greater stability in ER, OS, and traction coefficient. However, its solid equivalent (75% SB) showed a marked reduction when operated at a speed of 10 km h<sup>-1</sup> due to the overload admitted in the power train. The 40% HB configuration did not exhibit a behavior mathematically possible to be explained with a significant coefficient of determination, and its solid equivalent did not vary markedly in detriment to the study speed.

Through the results obtained experimentally, verifying operational and energy efficiency maximization with the correct dimensioning between ballast and operational speed is possible. It emphasized the highest performance levels when the set was configured with 75% HB on the parameters of strength and power in the drawbar, speed, fuel consumption, and thermal efficiency of the engine. Exceptionally due to the maintenance of the traction capacity in the largest loads, differing from the solid ballast that presented overload in the power train.

## CONCLUSIONS

1. Among the ballasting arrangements evaluated in the experiment, the use of hydraulic ballast in the fraction of 75% showed superiority to the solid configuration of 75% in terms of energy and operational performance, providing 5.58% more force in the drawbar, 14.49% operating speed and 13.57% less specific fuel consumption;
2. The increase in study speed by up to 8 km h<sup>-1</sup> increased strength, power, and yield in the drawbar, in addition to favoring the energy performance of the set with the increase in the thermal efficiency of the engine and reduction of specific consumption of fuel. However, the higher speeds resulted in overloading the powertrain when operated with the factory configuration and solid ballast.

## REFERENCES

- AHMADI, I. Development of a tractor dynamic stability index calculator utilizing some tractor specifications. **Turkish Journal of Agriculture and Forestry**, v. 37, n. 2, p. 203-211, 2013.
- AMERICAN SOCIETY OF AGRICULTURAL AND BIOLOGICAL ENGINEERS. ASABE D497.5. Agricultural machinery management data. **ASAE Standards**. St. Joseph, 2011.
- AMERICAN SOCIETY OF AGRICULTURAL AND BIOLOGICAL ENGINEERS. ASABE 496.3. Agricultural machinery management data. **ASAE standards**. St. Joseph, 2011.
- BATTIATO, A.; DISERENS, E. Tractor traction performance simulation on differently textured soils and validation: a basic study to make traction and energy requirements accessible to the practice. **Soil and Tillage Research**, v. 166, p. 18-32, 2017.
- BIETRESATO, M.; CALCANTE, A.; MAZZETTO, F. A neural network approach for indirectly estimating farm tractors engine performances. **Fuel**, v. 143, p. 144-154, 2015.
- DAMANAUSKAS, V.; JANULEVIČIUS, A. Differences in tractor performance parameters between single-wheel 4WD and dual-wheel 2WD driving systems. **Journal of Terramechanics**, v. 60, p. 63-73, 2015.
- FARIAS, M. S. D. *et al.* Air and fuel supercharge in the performance of a diesel cycle engine. **Ciência Rural**, v. 47, n. 6, 2017.
- FERREIRA, P. V. **Estatística experimental aplicada as ciências agrárias**. 1. Ed. Viçosa: UFV, 2018, 126 p.
- JANULEVIČIUS, A.; DAMANAUSKAS, V.; PUPINIS, G. Effect of variations in front wheels driving lead on performance of a farm tractor with mechanical front-wheel-drive. **Journal of Terramechanics**, v. 77, p. 23-30, 2018.
- JASPER, S. P. *et al.* Desempenho do trator de 157 kW na condição manual e automático de gerenciamento de marchas. **Scientia Agrária**, v.17, n.3, p.55-60, 2016.

- KUMAR, S.; NOORI, M. T.; PANDEY, K. P. Performance characteristics of mode of ballast on energy efficiency indices of agricultural tyre in different terrain condition in controlled soil bin environment. **Energy**, v. 182, p. 48-56, 2019.
- KUMAR, S. *et al.* Effect of ballasting on performance characteristics of bias and radial ply tyres with zero sinkage. **Measurement**, v. 121, p. 218-224, 2018.
- LACOUR, S. *et al.* A model to assess tractor operational efficiency from bench test data. **Journal of Terramechanics**, v. 54, p. 1-18, 2014.
- LOPES, J. E. *et al.* Operational and energy performance of the tractor-scarifier assembly: Tires, ballasting and soil cover. **Revista Brasileira de Engenharia Agrícola e Ambiental**, v. 23, n. 10, p. 800-804, 2019.
- LOVARELLI, D.; BACENETTI, J. Bridging the gap between reliable data collection and the environmental impact for mechanised field operations. **Biosystems engineering**, v. 160, p. 109-123, 2017.
- MARTINS, M. B. *et al.* Otimização energética de um trator agrícola utilizando normas técnicas em operações de gradagem. **Revista Engenharia na Agricultura**, v. 26, n. 1, p. 52-57, 2018.
- MAYET, C. *et al.* Influence of a CVT on the fuel consumption of a parallel medium-duty electric hybrid truck. **Mathematics and Computers in Simulation**, v. 158, p. 120-129, 2019.
- MOINFAR, A. *et al.* The effect of the tractor driving system on its performance and fuel consumption. **Energy**, v. 202, p. 117803, 2020.
- MONTEIRO, L. D. A. *et al.* Tractor drawbar efficiency at different weight and power ratios. **Revista Ciência Agronômica**, v. 44, n. 1, p. 70-75, 2013.
- MONTEIRO, L. D. A.; LANÇAS, K. P.; GUERRA, S. P. Performance of an agricultural tractor equipped with radial and bias ply tires on three levels of liquid ballast. **Engenharia Agrícola**, v.31, p.551-560, 2011.
- MONTGOMERY, D. C. **Introdução ao controle estatístico da qualidade**. 4. ed. Rio de Janeiro: LTC, 2004. 532 p.
- OECD – Organization for Economic Cooperation and Development. **Code 2: OECD standard code for the official testing of agricultural and forestry tractor performance**, 90 p, 2012.
- PRANAV, P. K.; PANDEY, K. P. Computer simulation of ballast management for agricultural tractors. **Journal of Terramechanics**, v. 45, n. 6, p. 185-192, 2008.
- SCHLOSSER, J. F. *et al.* Power hop in agricultural tractors. **Ciência Rural**, v. 50, p.20200199, 2020.
- SCHLOSSER, J. F. *et al.* Análise comparativa do peso específico dos tratores agrícolas fabricados no Brasil e seus efeitos sobre a seleção e uso. **Revista Ciência Rural**, v. 35, p. 92-97, 2005.
- SERRANO, J. M. *et al.* Tractor energy requirements in disc harrow systems. **Biosystems Engineering**, v. 98, p. 286-296, 2007.
- SHAFAEI, S. M.; LOGHAVI, M.; KAMGAR, S. An extensive validation of computer simulation frameworks for neural prognostication of tractor tractive efficiency. **Computers and Electronics in Agriculture**, v. 155, p. 283-297, 2018.
- ŠMERDA, T.; ČUPERA, J. Tire inflation and its influence on drawbar characteristics and performance–Energetic indicators of a tractor set. **Journal of Terramechanics**, v. 47, n. 6, p. 395-400, 2010.

